J. Appl. Comput. Mech., 7(3) (2021) 1826-1835
DOI: 10.22055/JACM.2021.36020.2819

ISSN: 2383-4536
jacm.scu.ac.ir

Shahid Chamran University of Ahvaz

Journal of Applied and Computational Mechanics

Research Paper

Numerical Investigation of Tissue-Temperature Controlled System in Thermal Ablation: A Finite Element Approach

Mridul Sannyal, Abul Mukid Mohammad Mukaddes

Department of Industrial and Production Engineering, Shahjalal University of Science and Technology, Sylhet, 3114, Bangladesh, Emails: sannyalmridul@gmail.com, mukaddes-ipe@sust.edu

Received January 04 2021; Revised July 04 2021; Accepted for publication July 09 2021.
Corresponding author: A.M.M. Mukaddes (mukaddes-ipe@sust.edu)

Abstract. In thermal ablation, several techniques of treating infected cell in human tissue are being used by the physicians. Transferring heat to the infected cell is one of them. The purpose of this research is to investigate the tissue-temperature controlled system in thermal ablation and compare with two different point heating processes, namely constant and step heating. For this purpose, the finite element model of Penne's bio-heat equation has been developed to measure the temperature within the two-dimensional tissue model embedded with a small tumor. The tissue temperature-controlled heating was designed to restrict the healthy tissue temperature below the damage threshold temperature. Using the temperature profile, tissue damage index was measured with the help of Arrhenius rate equation. The results show that the tissue temperature-controlled system reduces the temperature of healthy tissue nearby the infected cell to 40% compare to constant and step point heating. This system keeps the healthy tissue within the threshold value (43°C) up to 1000s when it is 100s for other two techniques. After 200s, healthy tissue nearby the infected cell start to damage for constant and step point heating. But temperature-controlled system always keep the healthy tissue safe. The results of this research conclude the temperature-controlled system a better heating technique to remove the infected cell. The information published in this paper will be helpful for the physicians and bio-medical engineers to treat the infected cell or to design medical equipment.

Keywords: Bio-heat Transfer, Finite Element Method, Tumor Ablation, Temperature –Controlled Heating, Step Heating.

1. Introduction

Physicians and bio medical engineers need to damage the infected cell of human tissue during different cancerous treatment. Generating high thermal energy within the infected cell is one of the way to damage them. Hyperthermia [1, 2] is a low temperature (42-45^{0}C)-high exposure time based treatment when thermal ablation is a high temperature (above 60^{0}C)-low exposure time based treatment. The later one is a technique to treat the tumor or any infected cell within human tissue by increasing the temperature in that cell above 60^{0}C [3, 4]. For this purpose, a high thermal energy needs to be generated within the infected region. The temperature of that region is thus raised to its damage range. Radiofrequency ablation (RFA), microwave ablation (MWA) [5, 6], high frequency based ultrasound [7] and laser ablation are commonly used as thermal ablation technique. Point heating, spatial heating or step heating are usually used to generate thermal energy at a desired level in those techniques. In the point heating process, the total thermal energy is deposited at the tumor site with the help of a heating probe or similar device. The target region is then heated to more than 60^{0}C within short times through heat conduction. Numerical study has found an inverse relationship between elevated temperature and exposure duration. For the same amount of tissue necrosis, high temperature needs low exposure time. On the contrary, low temperature needs high exposure time. Researchers have found that about 30 to 60 minutes needs to damage the infected cell at the temperature of around 42^{0}C-45^0 C. At temperature of above 60°C, the time that is required to achieve irreversible damage decreases exponentially [8]. The direct point heating cannot control the temperature of healthy tissue thus causes a risk of damaging healthy tissue nearby the infected cell. To overcome this adverse situation, some researchers used step heating technique [3], temperature-controlled technique [10-11] and spatial heating [9, 12, 13]. In step heating, for a recurring time interval, thermal energy is generated to the infected cell. The infected region is heated and then cooled again for a certain time. Another technique, tip temperature-controlled, predefines the maximum temperature of tip and beyond which, system stops to generate thermal energy. Most of the researchers, performed the experimental work and manually controlled the temperature of the applicators temperature using trial and error method. Though it is the more efficient approach, but it has some limitation as it only controls the temperature of the probe tip ignoring the temperature of the healthy tissue. Whatever techniques are used; precise acknowledgement of thermal history is utmost necessary for effective treatment. Many clinical experiments were performed for this purpose. Though experimental studies can provide more accurate result than numerical, but it requires suitable equipment and proper experimental setup. However numerical modelling can be an appropriate method towards that direction. Due to advances in computational technology, mathematical models has been

Published online: July 10 2021

gaining importance in the bio-heat transfer area. Moreover, due to non- invasive in nature and low cost, mathematical modelling again has gained more acceptance to researchers and scientists. In medical applications, the heat transfer phenomena in biological tissue not only need the experimental data but also basic mechanics of heat transport and mathematical modeling. For numerical study of thermal ablation technique, Penne's bio-heat transfer equation [14] is commonly used. Detail model building based on Penne's is shown by Jordan Hristov [15]. Mukaddes et al. [16] used this equation to study the skin burn using three dimensional model when Sannyal et al. [17] solved this equation using finite element method to investigate the tissue temperature under different heating conditions.

In this paper, a tissue temperature-controlled system has been proposed and compared with the methods available in the literature, namely with point heating and step heating. The tip temperature-controlled [18] system controls the tip temperature when the tissue temperature-controlled system controls the maximum temperature of the healthy tissue. Thereby, it ensures to keep the temperature of healthy tissue within the tolerable range [19] and treat the tumor cell without affecting the healthy tissue. The deposited thermal energy is controlled using the proportional-integral (PI) technique [19]. In the tissue temperature-controlled system, the applied external heating power will be automatically adjusted from the feedback of the healthy tissue's temperature. To examine the effectiveness of this technique, a two-dimensional finite element model for the human tissue (30mm x 30mm) with tumor in its center has been developed. To estimate the temperature profile, Penne's bio-heat equation was solved using finite element method. The analytical solution of one-dimensional [12, 15] and three-dimensional bio-heat equation [13] are available in the literature. The results of this study were validated with analytical and numerical one. The Arrhenius Rate Equation was used to evaluate the tissue thermal damage. The comparison of tissue temperature-controlled ablation technique was made perspective of temperature profile and tissue damage index. In both cases, the tissue temperature controlled technique performs better compare to the point and step heating.

2. Numerical Model

2.1 Tissue model and governing equation

A two dimensional tissue model of 30 mm X 30 mm including a circular tumor of 3.5 mm radius inside it was considered for the analysis. As shown in Fig. 1, x = 0 and x = 30 mm indicate the skin surface and body core respectively.

To estimate the temperature distribution inside the tissue model Pennes Bio-heat equation [20] expressed in Eq. (1) was used,

$$k\nabla^2 T + \omega_b \rho_b c_b (T_a - T) + Q_m + Q_r = \rho c \frac{\partial T}{\partial t} \tag{1}$$

Here ρ_b, c_b denote the density and specific heat of blood. While ρ, c is the density and specific heat of tissue, ω_b is the blood perfusion, T_a the known arterial temperature, T is unknown tissue temperature, Q_m is the metabolic heat generation, and Q_r the heat source due to spatial heating with respect to time t. To protect the skin surface cells, cold water was circulated over the skin surface. While the heat transfer coefficient of the cooling water is h_0 and T_0 is the temperature of cooling water. The body core temperature T_c is always constant. The boundary Γ_1 and Γ_1 were thermally insulated. Thus the boundary conditions used in this analysis, are shown in Eq. (2).

$$k\frac{\partial T}{\partial x}\eta_x + k\frac{\partial T}{\partial y}\eta_y = -h_0 (T_o - T) \quad \text{on } \Gamma_1 \tag{2a}$$

$$k\frac{\partial T}{\partial x}\eta_x + k\frac{\partial T}{\partial y}\eta_y = 0 \text{ on } \Gamma_2 \text{ and } \Gamma_3 \tag{2b}$$

$$T = T_c \text{ on } \Gamma_4 \tag{2c}$$

Here η_x and η_y are the unit normal vector along X and Y axis respectively.

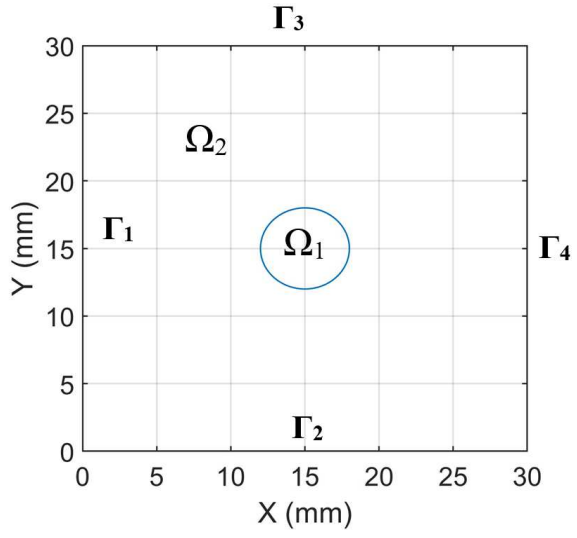

Fig. 1. Human Tissue Model

In this mathematical model a number of assumption was made. The tissue was assumed to be homogeneous and isotropic in each domain. Though the tissue properties like blood perfusion, thermal conductivity are temperature dependent, those material properties are considered constant inside each domain. During the simulation, in some cases the tissue temperature was high enough for melting of tissue. Such phase change heat transfer in analyzed during tissue heating by Abraham [21] and during tissue freezing by Li [22]. In this research such phase change was ignore, however tissue damage due to burn is considered. The initial temperature was considered as constant throughout the problem domain.

2.2 Constant Point Heating

Point heating is used to generate high thermal energy to a certain point, particularly in the tumor region [12, 13, 17]. In the computational analysis, this heating process was performed using the term used in Eq. (3),

$$Q_r = P(t)\delta(x,y) \tag{3}$$

where $P(t)$ is the heating power and δ is the Dirac delta function which has a value 1, at the desired point (15, 15), and zero otherwise.

2.3 Step Point Heating

The constant point heating might increase the temperature of the tumor tissue as well as healthy beyond it's critical value. There is a risk of damaging healthy tissue for this case. To avoid this, some researchers used the step point heating process for thermal ablation. Step point heating generates the heat transfer in the tumor region for a certain time interval and then it stops. It follows the following equation.

$$P(t) = \begin{cases} 2500\,Wm^{-2} & \text{for } t < 300s \text{ and } 500s < t < 800s \\ 0\ Wm^{-2} & \text{for otherwise} \end{cases} \tag{4}$$

2.4 Tissue Temperature-Controlled Point Heating

In this heating procedure, using a feedback system, the heating power is controlled by the temperature of the healthy tissue. If the healthy tissue reaches the critical temperature (damage threshold), the heat is stopped to generate automatically. Thereby this process ensures the healthy tissue to be always below the critical temperature and reduces the risk of damage. The Probable Integral (PI) method [17] as shown in equation (5) was used

$$P(t) = K_p\left(T_{set} - T_{tip}\right) + K_I \int \left(T_{set} - T_{tip}\right) dt \tag{5}$$

Here, $P(t)$ is the time dependent external heating power, which is adjusted over time. T_{set} is the predefined maximum temperature of healthy cells and T_{tip} is the maximum temperature of the healthy tissues at a certain time. K_p and K_I are constant which is considered as 0.17 and 0.0045 respectively [17].

2.5 Burn Quantification

To predict the thermal burn, several models have been developed by the researchers in the literature. Henriques model is one of them. From his experiment it was found that skin damage can be represented as chemical rate process. He insisted that Arrhenius rate equation can be used for the rate of tissue damage [23]. The developed equation for burn quantification is known as Henriques burn integral which is expressed as

$$\frac{\partial \alpha}{\partial t} = \int_0^t A e^{-\frac{\Delta E}{RT}} dt \tag{6}$$

where α is the damage index, A is the pre-exponential factor, ΔE is the activation energy, R is the molar gas constant (8.3144621 $Jkg^{-1}mole^{-1}$) and T is the skin temperature (K). In this study, we use the value of pre-exponential values and activation energy as ΔE=6.03E5 J/mole and A = 3.1E98 s^{-1} [23]. Again, fraction of tissue damage is calculated using the following expression [24].

$$\theta_d = 1 - e^{-\alpha} \tag{7}$$

2.6 Finite Element Discretization

Eq. 1 can be rewritten in simplified form as

$$k\frac{\partial^2 T}{\partial x^2} + k\frac{\partial^2 T}{\partial y^2} + C_w T_a + f = \rho c \frac{\partial T}{\partial t} \tag{8}$$

Here $C_w = \omega_b \rho_b c_b$ and $f = CT_a + Q_m + Q_r$

The weak form of Eq. 8 was derived using the weighted residual method in the following form

$$0 = \int_{\Omega_e} \left[W\rho c\frac{\partial T}{\partial t} + k\frac{\partial T}{\partial x}\frac{\partial w}{\partial x} + k\frac{\partial T}{\partial y}\frac{\partial w}{\partial y} + C_w WT - fW \right] dA - \oint_{\Gamma_e} W\left(k\frac{\partial T}{\partial x}\eta_x + k\frac{\partial T}{\partial y}\eta_y \right) ds \tag{9}$$

Here W is the weighted function. And using the finite element approximation finally a linear equation was derived of the following form

$$[\mathbf{C}]\{\dot{\mathbf{T}}\} + [\mathbf{K}]\{\mathbf{T}\} = \{F\}. \tag{10}$$

Here C is the capacitance matrix, K is the conductivity matrix, T is the unknown temperature and others are known vectors. Later time discretization method was used to solve this equation

Table 1. Typical Tissue Properties and Control Parameters.

Parameters	Symbol	Units
Thermal conductivity	k	0.5 W/(m.^{0}c)
Convection Coefficient	h_0	100 W/(m^2.^{0}c)
Environmental Temperature	T_0	15^{0}C
Temperature of the Artery	T_a	37^{0}C
Body core temperature	T_c	37^{0}C
Density of blood	ρ_b	1000 kg/m^3
Density of tissue	ρ	1000 kg/m^3
Specific heat of blood	c_b	4200 J/(kg.^{0}C)
Specific heat of tissue	c	4200 J/(kg.^{0}C)
Blood perfusion	ω_b	0.0005 m^3/s/m^3

2.7 Time Discretization

The popular Crank Nikolson method was used for time discretization of Eq. (10) as below

$$\left(C\frac{1}{\Delta T}+\varphi K\right)T^{n+1}=\left[C\frac{1}{\Delta T}-(1-\phi)K\right]T^{n}+F \tag{11}$$

Here $\dot{T}=(T^{n+1}-T^{n})/\Delta t$ and ϕ is the weighting factor which is considered as 0.5 in this paper.

3. Numerical Results and Discussion

Using the developed code, the governing equation is solved with the prescribed boundary conditions. Total heating time is 1000s with a time step of 0.25s. For initial condition temperature of the domain is considered 37^{0}C. The typical tissue properties used in this study is given Table 1 [25].

It is well known that the blood perfusion and metabolism of human tissue are greatly influenced by the presence of tumor. Hence for accurate prediction of temperature distribution it is necessary to use distinct material properties in tumor and healthy tissue. In this study we considered different properties for tissue and tumor. The blood perfusion and metabolism for Ω_1 and Ω_2 is considered as following [26].

$$\omega(x,y)=\begin{cases}0.002\,m^3/s/m^3 & \text{for } (x,y)\epsilon\Omega_1\\ 0.0005\,m^3/s/m^3 & \text{for } (x,y)\epsilon\Omega_2\end{cases} \tag{12}$$

$$Q_m(x,y)=\begin{cases}4200\,W/m^3 & \text{for } (x,y)\epsilon\Omega_1\\ 420\,W/m^3 & \text{for } (x,y)\epsilon\Omega_2\end{cases} \tag{13}$$

As scientists and researchers suggest that biological tissue can undergo up to 43^{0}C without any damage, our maximum prescribed value is considered as 43^{0}C. And 37^{0}C is used as the minimum prescribed value.

3.1 Comparison with Analytical and Numerical Model

Before using the computer program for further investigation, it is necessary to verify with the analytical solution. For this purpose, we develop a test problem and compare the result with analytical and numerical result found in the literature.

Boundary conditions for the test problem are as below

$$T=45^0C \text{ on } \Gamma_1 \quad T=37^0C \text{ on } \Gamma_4 \text{ and } k\frac{\partial T}{\partial x}\eta_x+\frac{\partial T}{\partial y}\eta_y=0 \text{ on } \Gamma_2 \text{ and } \Gamma_3 \tag{14}$$

For steady state case the analytical result is derived from the following expression [26]:

$$T(x)=T_a+\frac{(T_s-T_a)\sinh[\mu(L_1-x)]+(T_c-T_a)\sinh(\mu x)}{\sinh(\mu L_1)} \tag{15}$$

where, $\mu=\sqrt{(\omega_b\rho_b C_b)}$; T_s= Skin surface Temperature; L= Problem length along X- axis

The analytical result for the steady-state problem was calculated from Eq. (12), where domain length is 30 mm along x-axis and 30 mm along y-axis. Typical tissue properties used in this section are summarized in Table 1. In this case, heat production due to metabolism is ignored hence Q_m is considered as 0 W/m^3 and ω_b=0.0005 m^3/s/m^3

The steady state temperature in comparison with other analytical results is shown in Fig. 2. In addition to investigate the convergence performance of the solution, the comparison was performed for different mesh size of total number of elements. The right figure shows the mean absolute error for different element size, and it was found that the mean average error reduced significantly with the rise of total number of nodes. And the numerical results make a good agreement with the analytical one when the total number of nodes are 4900. That's why we used 4900 nodes for the further analysis. The transient solution at different distance from the skin surface with analytical and numerical results is shown in Table 2 while Y = 0 mm. It is apparent from this table that our result makes a better agreement with the analytical solution compare to RBF-MFS and Trefftz-FEM solution.

Table 2. FEM results of this study with other analytical and numerical solutions

Distance (mm)	FEM (This Study)	Analytical [24]	RBF-MFS [24]	Trefftz-FEM [24]
0	45	45	45	45
7.5	41.73	40.49	41.82	42.74
15	39.63	38.49	39.73	40.83
22.5	38.17	37.55	38.26	39.18
30	37	37	37	37

3.2 Results and Discussion

In this section, the temperature distribution and burn index due three different heating process has been discussed. The power of constant point heating is considered as $P(t)=2500\,Wm^{-2}$. For step point heating and tissue temperature controlled heating, the following parameters are used.

$$\text{Step point heating:}\quad P(t)=\begin{cases}2500\,Wm^{-2} & \text{for } t<300s \text{ and } 500s<t<800s\\ 0\ Wm^{-2} & \text{for otherwise}\end{cases} \tag{16}$$

$$\text{Tissue Temperature-Controlled:}\quad P(t)=K_p\left(T_{set}-T_{tip}\right)+K_I\int\left(T_{set}-T_{tip}\right)dt \tag{17}$$

3.2.1 Temperature Profile

Temperature profile for three different heating styles is shown in Fig. 3 (a-c) at 800s. Those three figures show a minimum temperature of almost 350C is at the skin surface and while at the body core temperature is almost 37^0C. Low temperature at the skin surface is as a result of cooling water. The computational results are showing that the minimum temperature exists on the skin surface and the maximum in the tumor region. The results shown in Fig. 3(a-b) depicts that, the temperature in the healthy tissue near the tumor region is about from 60^0C to 70^0C which is beyond burn threshold temperature 43^0C. Again Fig. 3(c) and numerical results depicts that the temperature of the healthy tissue even nearby tumor region, is always below the 45^0C.

Fig. 4 shows the maximum and minimum temperature for tumor and healthy tissue region at different time for three different heating processes. For constant point heating, temperature of both regions increases over time. For step heating, heating and cooling stages have been shown. In both heating process, same temperature pattern is shown in both tumor and healthy region. But for the temperature-controlled system, the temperature pattern within healthy tissue nearby the tumor region is drastically decreased.

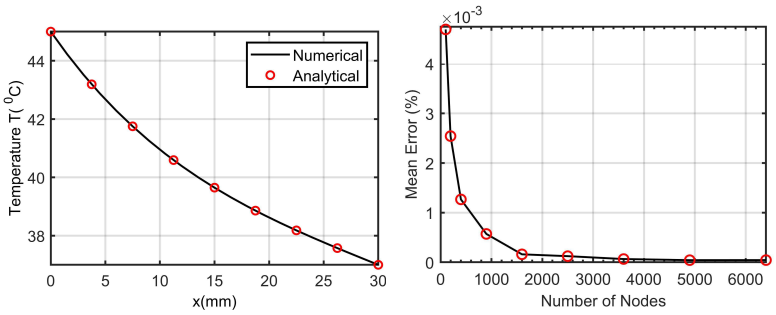

Fig. 2. Code Verification (Left: Comparison with analytical solution, Right: Mesh convergency)

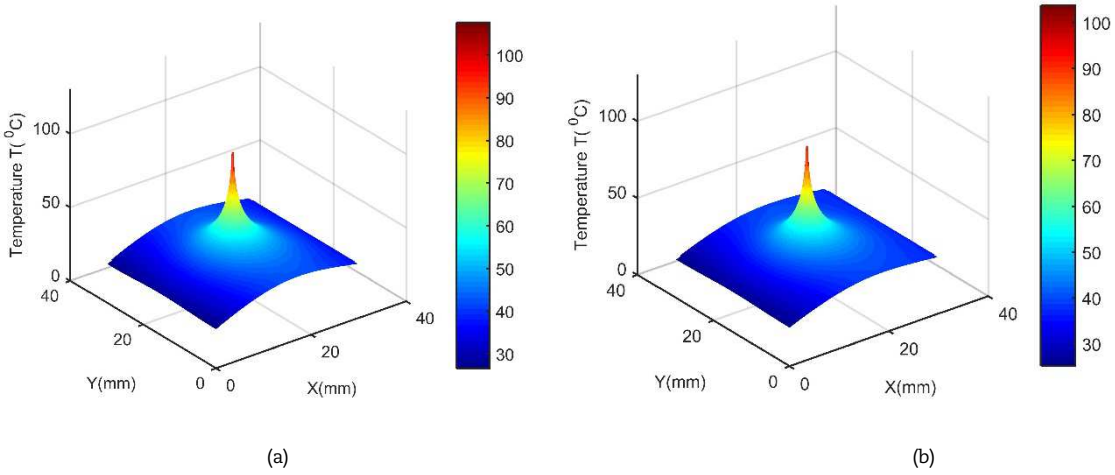

Fig. 3. Temperature Distribution in tissue subject to (a) Constant Heating (800s); (b) Step Heating (800s); (c) Control Heating (800s)

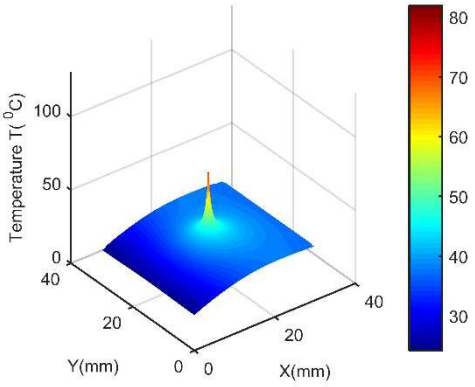

(c)

Fig. 3. Temperature Distribution in tissue subject to (a) Constant Heating (800s); (b) Step Heating (800s); (c) Control Heating (800s)

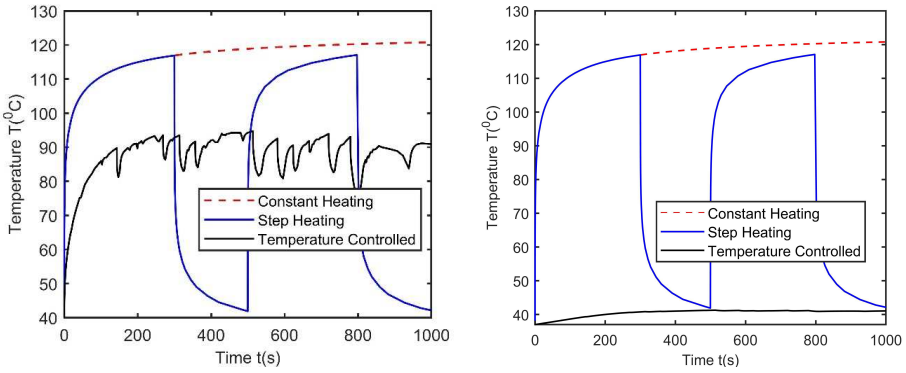

Fig. 4. Maximum and Minimum Temperature of (a) Tumor tissue and (b) Healthy Tissue

3.2.2 Isotherm Temperature Profile

Fig. 5, Fig. 6 and Fig. 7 show the isotherm for 42^{0}C and 45^{0}C for constant, step and control heating respectively. As irreversible damage does not start unless the temperature of the tissue crosses the threshold value so this isotherm, hence these figures will give a clear picture of the progression of damage. The red circle distinct the tissue from the tumor region. For constant heating both 42^{0}C and 45^{0}C contour crosses the tumor region and progresses towards the healthy cells after 100s. Same result is showing for step heating at 100s and 200s. However, after heating 400s, 45^{0}C isotherm remains within the tumor region as a result of first cooling down stage in step heating, where's for constant heating it still occupies a significant amount of healthy tissues. Situation becomes more severe for constant heating after 800s and 1000s. A significant portion of the healthy tissue is crossing the threshold value.

In case of temperature-controlled heating 45^{0}C always reaming within the tumor cells. Though area of the 42^{0}C isotherm goes beyond the target cells the progression is not as significant as constant or step heating. However, a common scenario is visible in all the figures and that is both isotherm tends to progress towards the body core compare to the skin surface. This is the result of skin cooling; the circulated water always keeps the skin surface temperature much lower than other tissues.

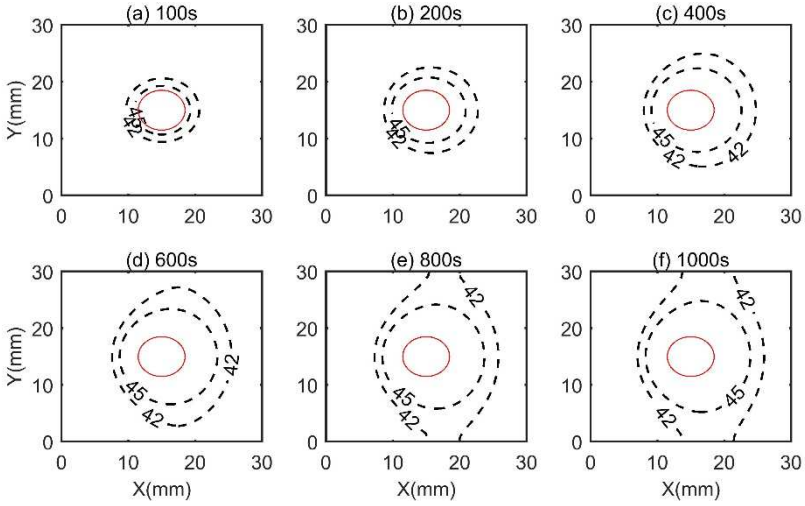

Fig. 5. Progression of 42^{0}C and 45^{0}C isotherm at different time for constant heating

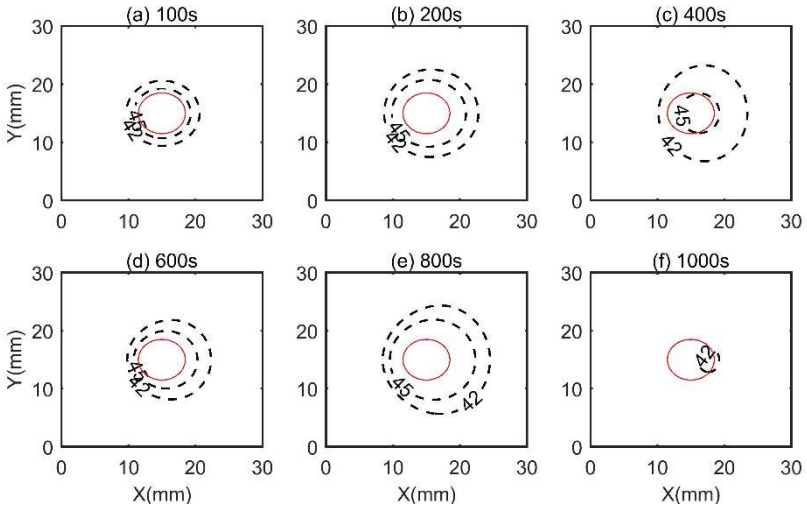

Fig. 6. Progression of 42°C and 45°C isotherm at different time for Step heating

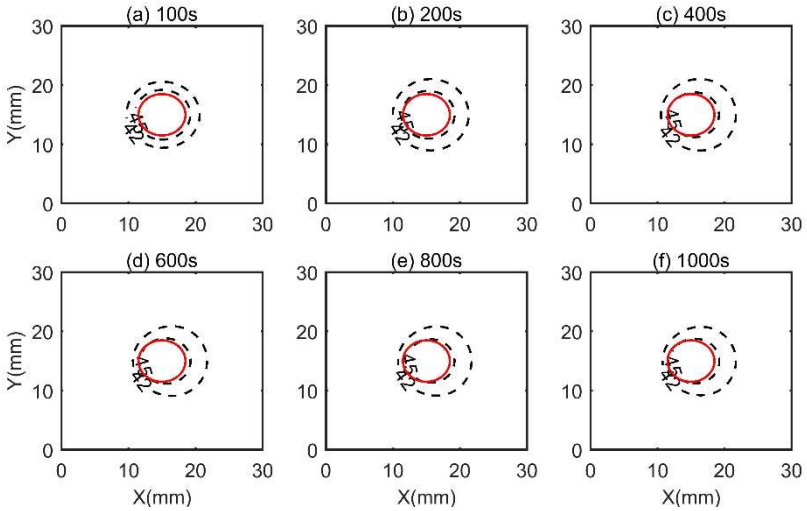

Fig. 7. Progression of 42°C and 45°C isotherm at different time for Control Heating

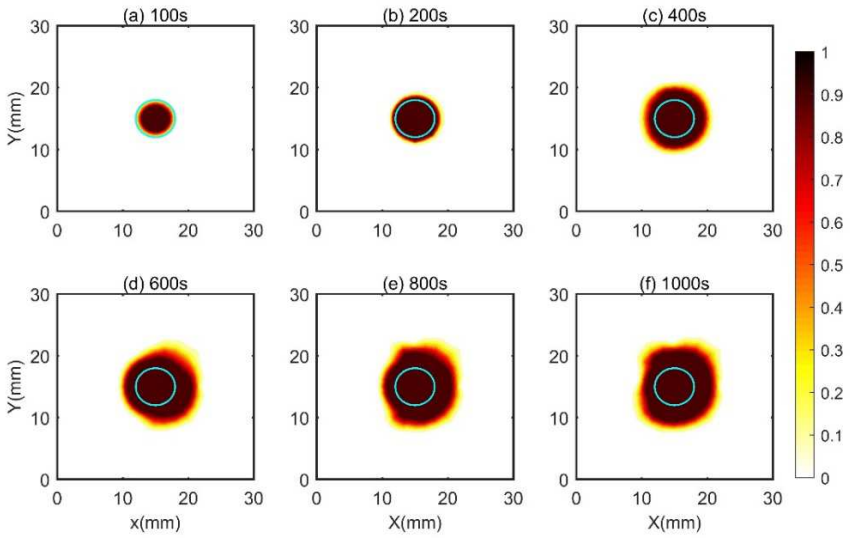

Fig. 8. Fraction of tissue damage for constant heating

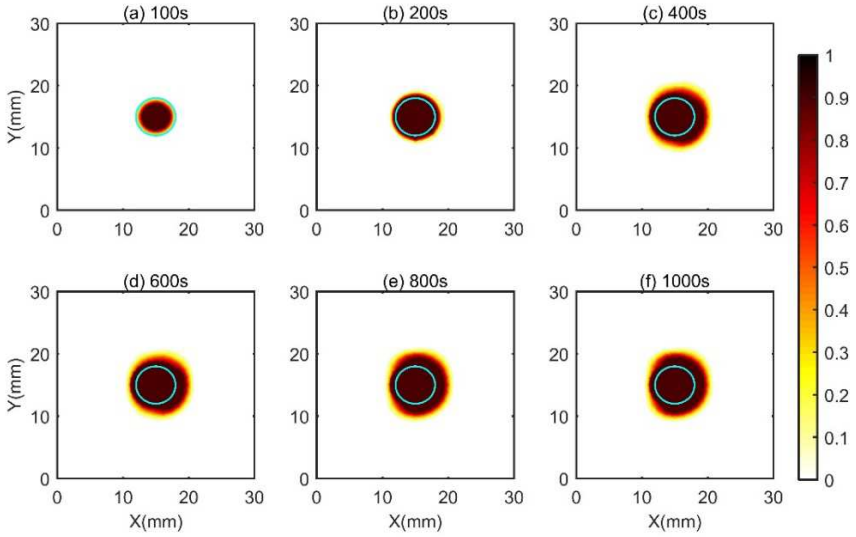

Fig. 9. Fraction of tissue damage for step heating

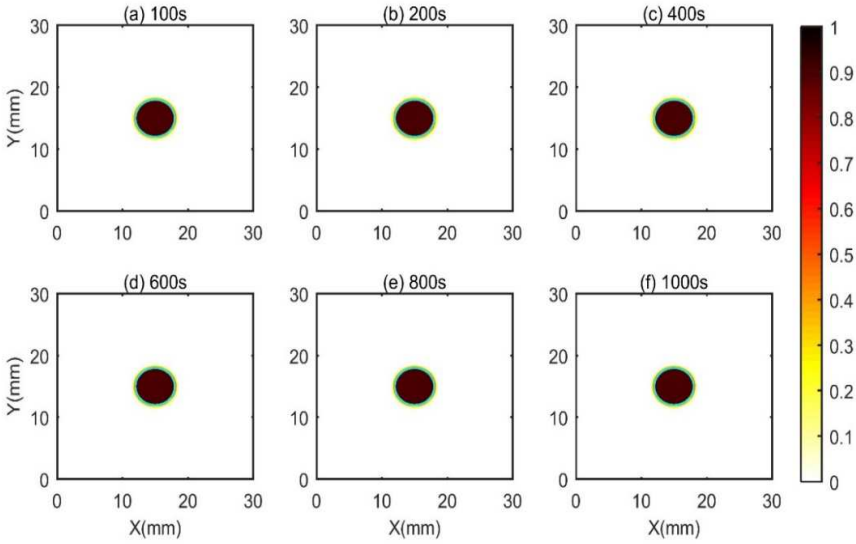

Fig. 10. Fraction of tissue damage for control heating

3.2.3 Tissue Damage Index

Fraction of tissue damage at different time for three different heating process is showing in Fig. 8, Fig. 9 and Fig. 10. The tumor region is highlighted using the circle within domain. In constant heating up to 100s all healthy cells remain safe. However, damage of the healthy cells starts afterward and at 800s and 1000s the situation becomes very severe. A greater portion of the healthy cells are damaged.

Though step heating shows better result concerning to safety of the healthy cells compared to constant heating but in 200s few cells still damages and for 400s to 800s this amount increases and results in undesirable damage of the functional tissues. However, the most desirable result is showing in Fig 10. For control heating, much of the tissue damage confines to the tumor region. A minor damage is observed to the healthy tissues close to the tumor. This is not surprising as we considered 45^0C as minimum prescribed value which is a little bit higher than the damage threshold value. Prescribing 42^0C as lower temperature value instead of 45^0C may lead to a batter scenario considering the safety of the healthy cells but it would definitely result in lower damage of the tumor cells comparing to the current setup. Considering 45^0C as the lower prescribed value fasters the tissue necrosis at tumor region. The effect of surface cooling is clearly visible in constant and step hating after 600s, 800s and 1000s. All of those figures are showing nearly identical interest in affecting the cells towards the body core and reluctant to the skin surface tissues, which are maintained at lower temperature compare to other using circulation of the cooling water towards the skin surface.

4. Conclusion

The finite element model and solution system have been developed to solve the Penne's bio-heat equation. Three heating process for thermal ablation were compared perspective of temperature distribution and damage index. In case of constant point and step point heating, the temperature of healthy tissue crosses the damage threshold value (43^0 C) at 100s and progresses. But tissue temperature-controlled system always keep the temperature of healthy tissue below the threshold value. Again damage of

healthy tissue nearby the tumor region started to damage after 200s for constant point and step heating. On the other hand, tissue temperature-controlled heating restricted the healthy tissue from damage even up to 1000s. The results indicate that, feedback system of tissue temperature can control the heat generation in the tumor region and thereby can save the healthy tissue nearby the infected cells. The information published in this paper will be helpful for the physicians and bio-medical engineer to treat the infected cell or to design medical equipment.

Author Contributions

A.M.M. Mukaddes initiated the research and designed the study while M. Sannyal, graduated from Shahjalal University of Science and Technology, carried out the background research and the numerical simulation and analyzed the results. Both author prepared, reviewed and approved the final version of the manuscript.

Conflict of Interest

The authors declared no potential conflicts of interest with respect to the research, authorship, and publication of this article.

Funding

The authors received no financial support for the research, authorship, and publication of this article.

Nomenclature

L_a	Characteristic Problem Length along X-axis [mm]	h_0	Ambient heat transfer coefficient [W/(m.^{0}C)]
L_b	Characteristic Problem Length along Y-axis [mm]	T_0	Temperature of the ambient air [^{0}C]
ω_b	Blood Perfusion rate [$m^3/s/m^3$]	P(t)	External heating power [W/m2]
ρ_b	Density of blood [kg/m3]	A	Pre-exponential factor [s^{-1}]
ρ	Density of Tissue [kg/m3]	ΔE	Activation energy [$Jmole^{-1}$]
c_b	Specific heat of blood [J/(kg.^{0}C)]	R	Molar gas constant [$Jkg^{-1}mole^{-1}$]
c	Specific heat of tissue [J/(kg.^{0}C)]	Ω	Tissue damage Index
k	Thermal conductivity [W/(m.^{0}C)]	Θ_d	Fraction of tissue damage
T_a	Temperature of the artery [^{0}C]	η_x	Unit normal vector along X-axis
T_c	Body core temperature [^{0}C]	η_y	Unit normal vector along Y-axis

References

[1] Simon, Caroline J., Damian E. Dupuy, and William W. Mayo-Smith, Microwave ablation: principles and applications, *Radiographics*, 25, 2005, S69-S83.
[2] Tang, Yun-dong, Tao Jin, and Rodolfo CC Flesch, Effect of mass transfer and diffusion of nanofluid on the thermal ablation of malignant cells during magnetic hyperthermia, *Applied Mathematical Modelling*, 83, 2020, 122-135.
[3] Saiyed, Z. M., S. D. Telang, and C. N. Ramchand, Application of magnetic techniques in the field of drug discovery and biomedicine, *BioMagnetic Research and Technology*, 1(1), 2003, 1-8.
[4] Chu, Katrina F., and Damian E. Dupuy, Thermal ablation of tumours: biological mechanisms and advances in therapy, *Nature Reviews Cancer*, 14(3), 2014, 199-208.
[5] Ortega-Palacios, Rocío, et al., Heat transfer study in breast tumor phantom during microwave ablation: Modeling and experimental results for three different antennas, *Electronics*, 9(3), 2020, 535.
[6] Tehrani, Masoud HH, et al., Use of microwave ablation for thermal treatment of solid tumors with different shapes and sizes—A computational approach, *PlosOne*, 15(6), 2020, e0233219.
[7] Chowdhury, Emdadul Haque, et al., Investigation on High Frequency Based Ultrasound Tissue Therapy by Finite Element Method, *2nd International Conference on Advanced Information and Communication Technology (ICAICT)*, IEEE, 2020.
[8] Nikfarjam, Mehrdad, Vijayaragavan Muralidharan, and Christopher Christophi, Mechanisms of focal heat destruction of liver tumors, *Journal of Surgical Research*, 127(2), 2005, 208-223.
[9] Rossmann, Christian, Frank Rattay, and Dieter Haemmerich, Platform for patient-specific finite-element modeling and application for radiofrequency ablation, *Visualization, Image Processing and Computation in Biomedicine*, 1(1), 2012, DOI: 0.1615/VisualizImageProcComputatBiomed.2012004898.
[10] Eick, Olaf J., Temperature controlled radiofrequency ablation, *Indian Pacing and Electrophysiology Journal*, 2(3), 2002, 66.
[11] Langberg, Jonathan J., et al., Temperature monitoring during radiofrequency catheter ablation of accessory pathways, *Circulation,* 86(5), 1992, 1469-1474.
[12] Deng, Zhong-Shan, and Jing Liu, Analytical study on bioheat transfer problems with spatial or transient heating on skin surface or inside biological bodies, *J. Biomech. Eng.*, 124(6), 2002, 638-649.
[13] Karaa, Samir, Jun Zhang, and Fuqian Yang, A numerical study of a 3D bioheat transfer problem with different spatial heating, *Mathematics and Computers in Simulation,* 68(4), 2005, 375-388.
[14] Pennes, Harry H., Analysis of tissue and arterial blood temperatures in the resting human forearm, *Journal of Applied Physiology*, 1(2), 1948, 93-122.
[15] Hristov, Jordan, Bio-heat models revisited: concepts, derivations, nondimensalization and fractionalization approaches, *Frontiers in Physics*, 7, 2019, 189.
[16] Mukaddes, Abul Mukid Md, et al., Finite Element-Based Analysis of Bio-Heat Transfer in Human Skin Burns and Afterwards, *International Journal of Computational Methods,* 2020, 2041010.
[17] Sannyal, Mridul, et al., Analysis of the effect of external heating in the human tissue: A finite element approach, *Polish Journal of Medical Physics and Engineering*, 26(4), 2020, 251-262.
[18] Wang, Xiaoru, et al., Numerical evaluation of ablation zone under different tip temperatures during radiofrequency ablation, *Math. Biosci. Eng.*, 16, 2019, 2514-2531.
[19] Yarmolenko, Pavel S., et al., Thresholds for thermal damage to normal tissues: an update, *International Journal of Hyperthermia*, 27(4), 2011, 320-343.
[20] Pennes, Harry H., Analysis of tissue and arterial blood temperatures in the resting human forearm, *Journal of Applied Physiology*, 1(2), 1948, 93-122.
[21] Abraham, J. P., and E. M. Sparrow, A thermal-ablation bioheat model including liquid-to-vapor phase change, pressure-and necrosis-dependent perfusion, and moisture-dependent properties, *International Journal of Heat and Mass Transfer*, 50(13-14), 2007, 2537-2544.
[22] Li, Fang-fang, Jing Liu, and Kai Yue, Exact analytical solution to three-dimensional phase change heat transfer problems in biological tissues subject to freezing, *Applied Mathematics and Mechanics*, 30(1), 2009, 63-72.
[23] Henriques, F.C., Jr., Studies of Thermal Injuries V. The Predictability and the Significance of Thermally Induced Rate Processes Leading to Irreversible Epidermal Injury, *Archives of Pathology*, 43, 1947, 489-502.
[24] Davis, Trevor E., et al., Bio-Heat Transfer in Various Transcutaneous Stimulation Models, *International Journal of Medical, Health, Biomedical, Bioengineering and Pharmaceutical Engineering*, 8(9), 2014, 617-623.

[25] Carslaw, Horatio Scott, and John Conrad Jaeger, *Conduction of heat in solids*, Clarendon Press, 1992.
[26] Cao, Leilei, Qing-Hua Qin, and Ning Zhao, An RBF–MFS model for analysing thermal behaviour of skin tissues, *International Journal of Heat and Mass Transfer*, 53(7-8), 2010, 1298-1307.
[27] Shen, Wensheng, Jun Zhang, and Fuqian Yang, Modeling and numerical simulation of bioheat transfer and biomechanics in soft tissue, *Mathematical and Computer Modelling*, 41(11-12), 2005, 1251-1265.
[28] Tungjitkusolmun, Supan, et al., Three-dimensional finite-element analyses for radio-frequency hepatic tumor ablation, *IEEE Transactions on Biomedical Engineering*, 49(1), 2002, 3-9.
[29] Haemmerich, Dieter, and John G. Webster, Automatic control of finite element models for temperature-controlled radiofrequency ablation, *Biomedical Engineering Online*, 4(1), 2005, 1-8.
[30] Cao, Leilei, Qing-Hua Qin, and Ning Zhao, An RBF–MFS model for analysing thermal behaviour of skin tissues, *International Journal of Heat and Mass Transfer*, 53(7-8), 2010, 1298-1307.
[31] Liu, Jing, and Lisa X. Xu, Boundary information based diagnostics on the thermal states of biological bodies, *International Journal of Heat and Mass Transfer*, 43(16), 2000, 2827-2839.
[32] Davis, Trevor E., et al., Bio-Heat Transfer in Various Transcutaneous Stimulation Models, *International Journal of Medical, Health, Biomedical, Bioengineering and Pharmaceutical Engineering*, 8(9), 2014, 617-623.
[33] Stoll, Alice M., and Leon C. Greene, Relationship between pain and tissue damage due to thermal radiation, *Journal of Applied Physiology*, 14(3), 1959, 373-382.

ORCID iD

Mridul Sannyal https://orcid.org/0000-0001-5040-5549
Abul Mukid Mohammad Mukaddes https://orcid.org/0000-0001-7965-4602

How to cite this article: Sannyal M., Mukaddes A.M.M. Numerical Investigation of Tissue-Temperature Controlled System in Thermal Ablation: A Finite Element Approach, *J. Appl. Comput. Mech.*, 7(3), 2021, 1826–1835.
https://doi.org/10.22055/JACM.2021.36020.2819